Differential FeS cluster photodamage plays a critical role in regulating excess electron flow through photosystem I

Arjun Tiwari [13], Fikret Mamedov[2], Duncan Fitzpatrick [1], Sanna Gunell [1], Mikko Tikkanen [1] and Eva-Mari Aro [13]

[1]Molecular Plant Biology unit, Department of Life Technologies, University of Turku, FI-20014 Turku, Finland; [2]Molecular Biomimetics, Department of Chemistry- Ångström Laboratory, Uppsala University, Box 523, SE-75120 Uppsala, Sweden

[3]Correspondence addressed to Eva-Mari Aro, Email: evaaro@utu.fi; and Arjun Tiwari Email: arjun.tiwari@utu.fi

Orcid ID: Eva-Mari Aro - 0000-0002-2922-1435, Arjun Tiwari - 0000-0001-9095-2061

Summary statement: Photosystem I photoinhibition and differential damage of FeS clusters under high light is a natural phenomenon in angiosperms and controls electron flow to molecular oxygen whilst maintaining optimal CO_2 assimilation rates.

Keywords: PSI acceptor side limitation, PSI photoinhibition, photoprotection, ROS production, EPR spectroscopy, MIMS

Differential FeS cluster photodamage plays a critical role in regulating excess electron flow through photosystem I

ABSTRACT

The photosynthetic electron transport flux from photosystem (PS) I is mainly directed towards linear electron transport (LET), but a fraction is always shared between alternative electron transport (AET) and cyclic electron transport (CET). Although the electron transfer from P700 to ferredoxin (Fd), via phylloquinone and the FeS_X, FeS_B and FeS_A clusters, is well characterized, a regulatory role of these redox intermediates in the delivery of electrons from PSI to LET, AET and CET under environmental stress remains elusive. Here, we provide evidence for sequential damage to PSI FeS clusters under high light (HL), and subsequent slow recovery under low light

in *Arabidopsis thaliana*. WT showed 10-35% photodamage to their $FeS_{A/B}$ with increasing HL duration, without much effect on P700 oxidation capacity, FeS_X function and CO_2 fixation rate, and without additional oxygen consumption (O_2 photoreduction). Parallel $FeS_{A/B}$ cluster damage in the *pgr5* mutant was more pronounced, 50-85%, probably due to weak photosynthetic control and low non-photochemical quenching. Such severe electron pressure on PSI was also shown to damage the FeS_X clusters, with a concomitant decrease in P700 oxidation capacity and a decrease in thylakoid-bound Fd in the *pgr5* mutant. The results from WT and *pgr5* plants reveal a controlled damage of PSI FeS clusters under HL. In WT plants, this favors the electron transport to LET over AET by intact PSI centres, thereby preventing ROS production and probably promoting harmless charge recombination between $P700^+$ and FeS_X^- as long as the majority of $FeS_{A/B}$ clusters remain functional.

INTRODUCTION

Photosynthesis is one of the most fundamental processes in biology, providing energy and oxygen to sustain life on Earth. Photosynthetic light reactions are particularly vulnerable to environmental stress, including high light (HL) conditions. Depending on environmental and metabolic conditions, the sustenance of CO_2 fixation rates and optimal metabolism requires also alternative electron transport pathways that divert electrons from linear electron transfer (LET) pathway to molecular oxygen (O_2) and quinones or back from PSI to cytochrome b_6f (Cytb_6f), instead of reaching $NADP^+$. Also, it is of particular interest that within the PSI complex, there are two separate internal electron transfer routes, referred to as A-branch and B-branch, with different redox potentials of phylloquinone (PhQ)[1]. It was hypothesized that A-branch is providing a photoprotective back-reaction pathway but the conditions and mechanisms triggering such a protection have remained unclear.

At times, LET exceeds the capacity of the PSI acceptors to handle the incoming electrons, increasing the probability of electron transfer to O_2. This results in the generation of superoxide ($O_2^{\bullet-}$) and hydrogen peroxide (H_2O_2) at PSI acceptor side, activating the chloroplast antioxidant machinery to counteract oxidative damage and allowing O_2 to act as a safe electron sink via the Mehler reaction[2–4]. Although the well-known water-water cycle (WWC)[2,4] is universal in oxygenic photosynthetic organisms, and particularly in flowering plants, its capacity in utilizing excess electrons may vary. Indeed, the specificities and regulation of electron flow from primary charge separation (photooxidation of P700) in PSI to O_2, have remained largely unstudied in terms of PSI photoprotection. Electron transfer from PSI to molecular oxygen, without generation of ROS, is efficiently mediated by flavodiiron proteins, but these have disappeared during the evolution of flowering plant angiosperms[5,6]. Cyclic electron transfer around PSI, on the other hand, has been suggested to be crucial for maintaining optimal energy budget for photosynthesis[7,8] and for maintaining redox homeostasis to prevent PSI photoinhibition[9,10].

There are also numerous short-term photoprotective mechanisms that are activated rapidly when plants are exposed to HL, such as energy-dependent non-photochemical quenching of

excess excitation energy (NPQ)[11–13], lumen protonation-induced limitation of LET by Cytb_6f (photosynthetic control)[14,15] or redirection of excess excitation energy towards PSI[16]. Despite effective NPQ and photosynthetic control, the over-reduction and consequent damage to PSI FeS clusters is common in flowering plant chloroplasts under highly reducing environmental conditions[16–19]. However, the differential damage and role of the three consecutive PSI FeS clusters (X, A and B) has remained elusive.

Here, the loss of P700 oxidation capacity (decrease of Pm) and the damage of FeS_X and $FeS_{A/B}$ clusters were independently assessed from the GL-exposed and moderately HL-treated WT and *pgr5* mutants of *Arabidopsis thaliana* (hereafter *Arabidopsis*). Our results show a photodamage to the PSI $FeS_{A/B}$ clusters, which in WT increased with duration of HL (up to 43% in 120 min), but without noticeable effects on P700 photooxidation capacity (Pm) or the function of the FeS_X clusters. The *pgr5* mutant showed a difference from WT both in growth light (GL) and during the HL exposure. In GL, *pgr5* exhibited a significantly lower capacity for P700 photooxidation and $FeS_{A/B}$ reduction than WT, and during the HL treatment, there was a severe damage to P700 photooxidation and to both the $FeS_{A/B}$ and FeS_X cluster reduction capacities, ultimately leading a release of most of the Fd from the thylakoid membrane. Sequential damage of PSI redox cofactors under HL is shown to affect the delivery of electrons to different pathways from PSI.

RESULTS

The discovery of persistence of the P700 oxidation (maximal Pm) in relation to the integrity of PSI $FeS_{A/B}$ clusters between WT and the *pgr5* mutant[16] prompted us to explore in detail this fundamental controversy and to clarify the consequences on the partitioning of electrons from PSI to different acceptors, including atmospheric O_2 and CO_2.

Change in P700, FeS clusters and fluorescence after GL and HL treatments

First, the dark-acclimated parameters of PSI and PSII were examined and compared between the WT and the *pgr5* mutant from constant growth light (GL) (120 µmol photons m^{-2} s^{-1}) (**Fig. 1**). The leaves from *pgr5* mutant demonstrated ca. 20% lower level of the maximally oxidized P700 than the WT plants (**Fig. 1A**). The maximum oxidation of P700 (P_m) was induced by a strong saturating pulse under far red background light. We next isolated the thylakoids from WT and *pgr5* plants and subjected them to measurements of functional FeS clusters ($FeS_{A/B}$) using EPR spectroscopy at 16 K. The quantity of photo-reducible $FeS_{A/B}$ clusters, expressed on chlorophyll basis, was in the *pgr5* mutant plants about 64% of that in the WT from similar growth conditions (**Fig. 1B,C**). Conversely, there was no or only minor differences in the photosynthetic efficiency (Fv/Fm) of PSII (**Fig. 1D**) or partial photochemical quenching parameter in the dark (qL_D) (**Fig. 1E**), but both the minimum (F_0) (**Fig. 1F**) and maximum fluorescence (F_m) (**Fig. 1G**) were somewhat lower in *pgr5* plants compared to control WT grown under similar GL conditions. This corroborates our previous report[16] showing an unchanged PSI/PSII ratio between WT and *pgr5* mutants measured by room temperature EPR spectroscopy of oxidized tyrosine D and P700 signals.

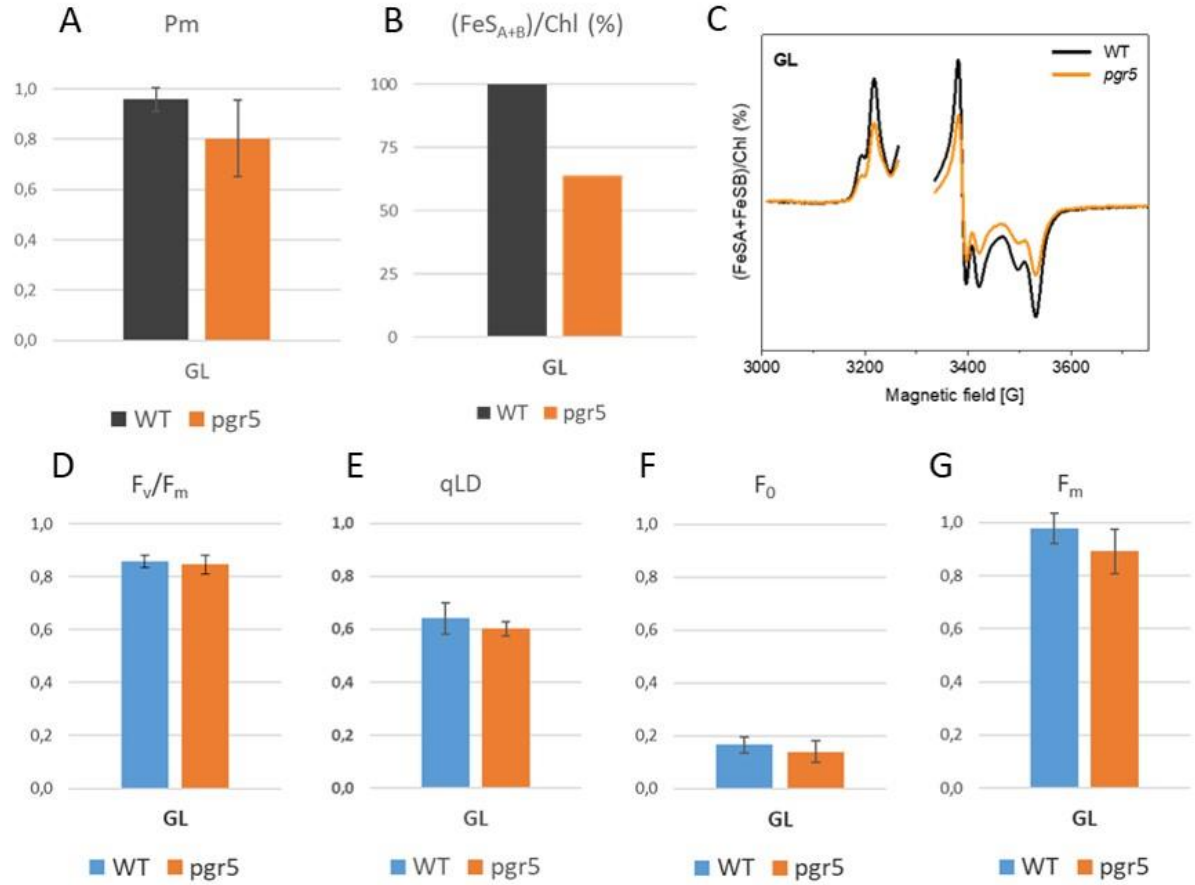

Figure 1: PSI and PSII parameters of WT and the *pgr5* mutant acclimated to GL. A, The maximum amount of oxidizable P700 (P_m) was determined by applying 10 s far-red illumination followed by a saturating pulse to 30 min dark incubated leaves n=8. **B**, quantification of $FeS_{A/B}$ from thylakoids isolated from GL plants (on Chl basis). **C**, EPR spectra of $FeS_{A/B}$ clusters from isolated thylakoids of WT and *pgr5* mutant plants measured at 16 K by photoreduction for 6 min using white actinic light. **D**, photosynthetic efficiency of PSII (F_v/F_m) n=8. **E**, Partial photochemical quenching parameter (qL_D) in dark acclimated state n=5. **F**, Minimal fluorescence (F_0) after 30 min dark incubation n=8. **G**, Maximum fluorescence of PSII after 30 min dark incubation (F_m) of GL WT and pgr5 mutant leaves n=5. Data are presented as mean values ±SD for (n) biological replicates. The FeS cluster data was obtained by combining two sets of thylakoids isolated from individually HL-treated plants (15-20 plants) in order to reach high enough chlorophyll concentration for EPR measurements.

Second, the leaves were exposed to HL treatment followed by analysis of PSI and PSII parameters. During HL illumination, the *pgr5* mutant plants showed a strong decrease in Pm levels, as determined by the Dual Pam program (**Fig. 2A**), and in the amount of photoreducible $FeS_{A/B}$ clusters (**Fig. 2B,C**). In contrast to *pgr5*, HL treatment of WT leaves did not significantly affect the Pm levels (as shown in **Fig. 2A**), but caused a gradual photodamage of $FeS_{A/B}$ clusters with increasing exposure time to HL (**Fig. 2B,C**). The amount of photoreducible $FeS_{A/B}$ clusters, expressed on chlorophyll basis, showed only a slight decrease in WT plants during the first 30

min of HL treatment, but more substantial decrease was recorded after 60- and 120-min of HL treatment (**Fig. 2B,C**). These results indicate that the PSI $FeS_{A/B}$ clusters are the most vulnerable primary targets of PSI photodamage during HL illumination, and that the damage to the P700 photooxidation capacity (Pm level) is only a subsequent event. This suggests a completely new aspect for the investigation of PSI photoinhibition mechanisms, which is not only present in the *pgr5* mutant but also in the WT plants. Indeed, the HL treatment induced a clear loss of functional $FeS_{A/B}$ clusters also in WT (**Fig. 2B**; 60 and 120 min) which, however, did not affect the P700 oxidation capacity (Pm) (**Fig. 2A**).

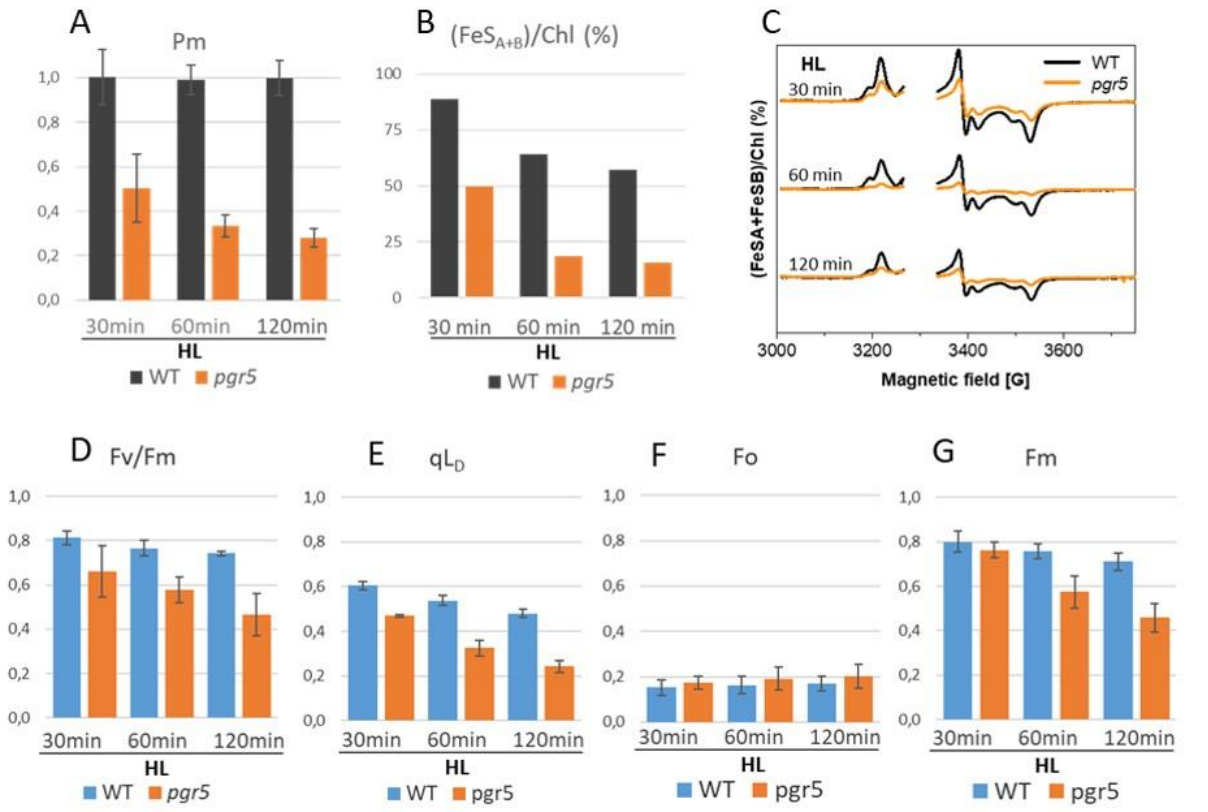

Figure 2: PSI and PSII parameters after the HL treatments HLl for 30, 60 and 120 min of GL-grown WT and *pgr5* plants. HL treatments were given to intact leaves. The Pm and fluorescence parameters were recorded after 30 min dark incubation of leaves. The FeS clusters were measured from thylakoids isolated from HL treated leaves and expressed as a percentage of their respective GL value (see Figure 1). **A**, The maximum amount of oxidizable P700 (P_m) was determined by applying 10 s far-red illumination followed by a saturating pulse n=8; **B**, quantification of $FeS_{A/B}$ on Chl basis; **C**, EPR spectra of $FeS_{A/B}$ clusters, measured at 16 K by photoreduction for 6 min using white actinic light; **D**, photosynthetic efficiency (F_v/F_m) n=8; **E**, Partial photochemical quenching parameter (qL_D) in dark acclimated state n=5; **F**, Minimal fluorescence (F_0) n=8 and **G**, Maximum fluorescence of PSII (F_m) n=5. Data are presented as mean values ±SD for (n) biological replicates. The FeS cluster data was obtained by combining two sets of thylakoids isolated from individually HL-treated plants (15-20 plants) in order to reach high enough chlorophyll concentration for EPR measurements.

Fluorescence parameters were likewise modulated in HL illuminated leaves. The F_v/F_m parameter decreased more during the first 30 min of HL treatment in *pgr5* than in WT leaves (**Fig. 2D**) compared to respective reference values in GL (**Fig. 1D**). Interestingly, the prolonged duration of HL to 60 and 120 min did significantly further modify the F_v/F_m values in WT or *pgr5* leaves. The photochemical quenching coefficient in dark-acclimated leaves (qL_D)[20], based on the PSII lake model relative to the references (WT or *pgr5* in GL, see Fig. 1E) was also calculated. In both HL-treated WT and *pgr5* plants, the qL_D value decreased considerably during the first 30 min of HL illumination compared to the reference values in GL. However, decrease was clearly more in pgr5 than in WT. Prolonged HL illumination of 60 and 120 min slightly decreased qL_D values in WT but did not further change qL_D values significantly in the *pgr5* mutant (**Fig. 2E**). F_0 fluorescence, however, increased in HL particularly in *pgr5* (**Fig. 2F**), which probably resulted from a change in the connectivity between PSII and the LHCII antenna[21]. In WT leaves, the F_m values decreased significantly during the first 30 min of HL illumination and even more in the pgr5 leaves (**Fig. 2G**), with respect to the control values in GL (**Fig. 1G**). Prolonged illumination for 60 and 120 min, did not induce any significant further changes of the Fm values in WT or *pgr5*.

Recovery of PSI and PSII from HL-treatments during 24 h

We have previously reported a complete recovery of photosynthetic electron transfer processes and CO_2 assimilation rates within 7 days following the HL-induced damage in intact *pgr5* plants[22]. Here, however, the damage of the PSI FeS clusters in HL-treated WT appeared as a novel phenomenon. Therefore, the possibility of repair of the PSI FeS clusters in WT and *pgr5,* together with other parameters of PSI and PSII, were investigated from HL-treated detached leaves after floating them for one extra day on water under dim room light. Such a compromise in the length of the recovery period was necessary to guarantee the visual freshness of leaves. Subsequently, the redox kinetics of P700 (photooxidation and re-reduction) was investigated by applying the following illumination protocol: firing first a single turnover saturating light pulse (ST) followed by a multiple turnover (MT) saturating pulse of actinic light under continuous background of far red (FR) light. The P700 redox kinetics under FR light (**Fig. 3A**) or the Pm level in WT (**Fig. 3B**) were not affected by the HL-treatments and neither showed any differences after floating the leaves for 24 h under dim room light (**Fig. 3A-B**). However, after 24 h recovery, a small increase was observed in photooxidation capacity of the $FeS_{A/B}$ clusters in 60 and 120 min HL-treated WT leaves (**Fig. 3C**, grey and black shades, respectively). Similar increase was observed in the F_v/F_m values of WT leaves after 24 h recovery in very dim light (**Fig. 3D**), whereas the F_m values in WT showed more substantial recovery (**Fig. 3F**), but the F_0 (**Fig. 3E**) levels remained unchanged after 24 h recovery period.

Unlike WT, the *pgr5* leaves showed a clear decline in P700 oxidation capacity (**Fig. 3G**, broken lines) and Pm levels (Fig. 3H, light blue shades) following the HL treatments of 30, 60 and 120 min (**Fig. 3G,H**). During subsequent recovery for 24h in dim light, we observed an increase in P700 oxidation levels during the redox kinetics measurements (**Fig. 3G,** solid lines) and a noteworthy increase in the Pm levels of *pgr5* leaves (**Fig. 3H,** dark blue shades). Similarly, the PSI $FeS_{A/B}$ clusters of HL-treated *pgr5* leaves, measured at 16K from isolated thylakoids, showed approximately 10-15% recovery in photoreduction after 24 h recovery in dim light (**Fig. 3I**).

Partial recovery of the PSII quantum yield was also observed in *pgr5* leaves after 24 h recovery in dim light (**Fig. 3J**). In contrast to WT, F_0 was slightly higher in *pgr5* leaves after 24 h recovery compared to that measured the same day after the HL treatment (**Fig. 3K**). However, Fm showed a substantial recovery after 24 h recovery in *pgr5* leaves as well (**Fig. 3L**).

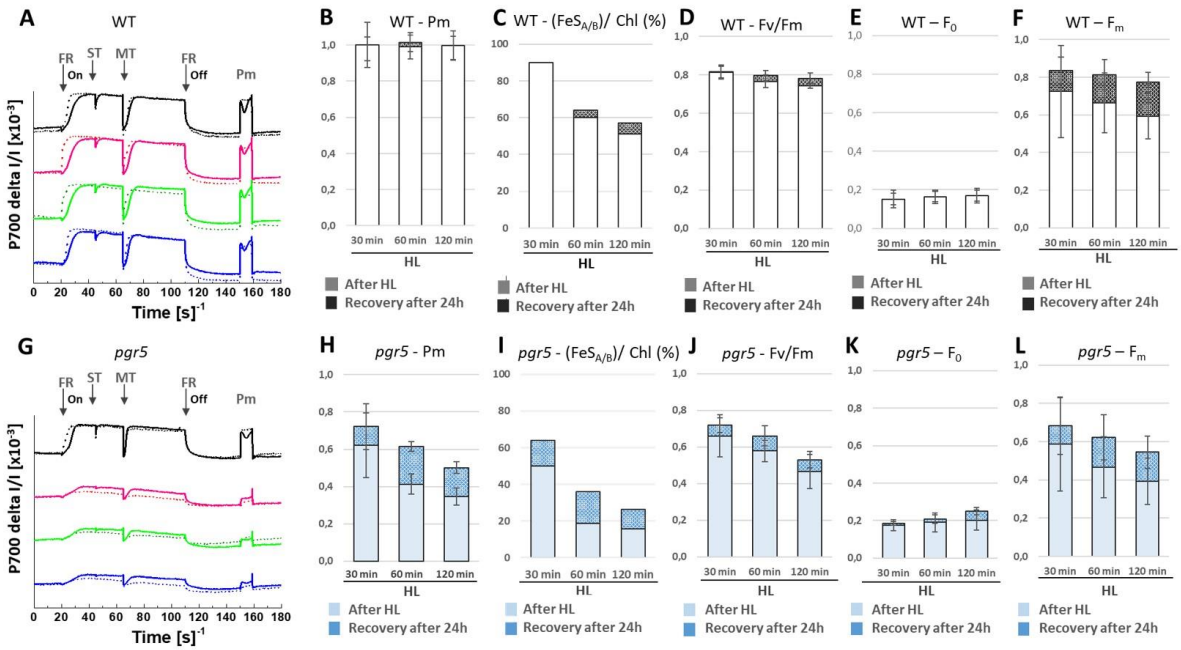

Figure 3. **Recovery of PSI and PSII from 30, 60 and 120 min HL-induced photoinhibition (light shades, value taken from Figure 2) during 24 hours in dim light (2 µmol photons m^{-2} s^{-1}, dark shades).** Pm and fluorescence parameters were recorded from intact leaves and the $FeS_{A/B}$ clusters from isolated thylakoids. Parameters after HL treatments are shown as uncoded bars (White for WT and light blue for pgr5) and after 24-h recovery as pattern bars (black for WT and blue for pgr5). **A**, WT P700 redox kinetics measured from GL- and HL-treated leaves (dotted lines, measured after 30 min dark incubation) and after 24-h recovery in very dim light (solid lines) n=5. **B**, WT Maximally oxidized P700 (Pm) n=8. **C**, WT PSI-$FeS_{A/B}$ clusters. **D**, WT Fv/Fm n=8. **E**, WT Minimal fluorescence (F_0) n=8. **F**, WT Maximum fluorescence of PSII (F_m) n=8. **G**, *pgr5* P700 redox kinetics measurements from GL- and HL-treated leaves (dotted lines) and after subsequent recovery for 24-h (solid lines) n=5. **H**, *pgr5* Pm n=8. **I**, *pgr5* PSI-$FeS_{A/B}$ clusters. **J**, *pgr5* F_v/F_m n=8. **K**, *pgr5* F_0 n=8. **L**, *pgr5* F_m n=8. Data are presented as mean values ±SD for (n) biological replicates. The FeS cluster data was obtained by combining two sets of thylakoids isolated from individually HL-treated plants (15-20 plants) in order to reach high enough chlorophyll concentration for EPR measurements.

Fate of PSI FeS_X clusters during HL illumination

Previously, we hypothesized that the damage to PSI FeS_X clusters prevents P700 photooxidation in the *pgr5* mutant, whereas in WT *Arabidopsis* the back reaction with functional FeS_X clusters maintains stable P700 photooxidation capacity[16]. Since our toolbox did not allow direct measurement of the functional FeS_X clusters and thereby to assess their role in PSI photoinhibition, we took advantage of the well-known fact that the FeS_X cluster is required to mediate electron transfer from the reduced P700 to an artificial PSI electron acceptor MV[23,24]. To apply this method, the leaves of GL-grown and HL-treated WT and *pgr5* mutant plants were incubated either in deionized water alone or with 1 µM MV, for 2h in darkness. The redox

kinetics of P700 (photooxidation and re-reduction) were then investigated as described in (**Fig. 3A**). The addition of MV increased the rate and extent of P700 oxidation under FR light in leaves of WT plants grown under GL as well as in leaves subsequently treated with HL for 30, 60 and 120 min (**Fig. 4A,B**). The presence of MV enhanced the oxidation of P700 both upon the onset of FR light and during subsequent re-reduction caused by ST and MT pulses of actinic light, in both the GL-grown and the HL-treated leaves of WT plants (**Fig. 4B**). This indicated that the moderate damage to $FeS_{A/B}$ clusters in WT (**Fig. 2B**) did not interfere with the electron transfer to MV.

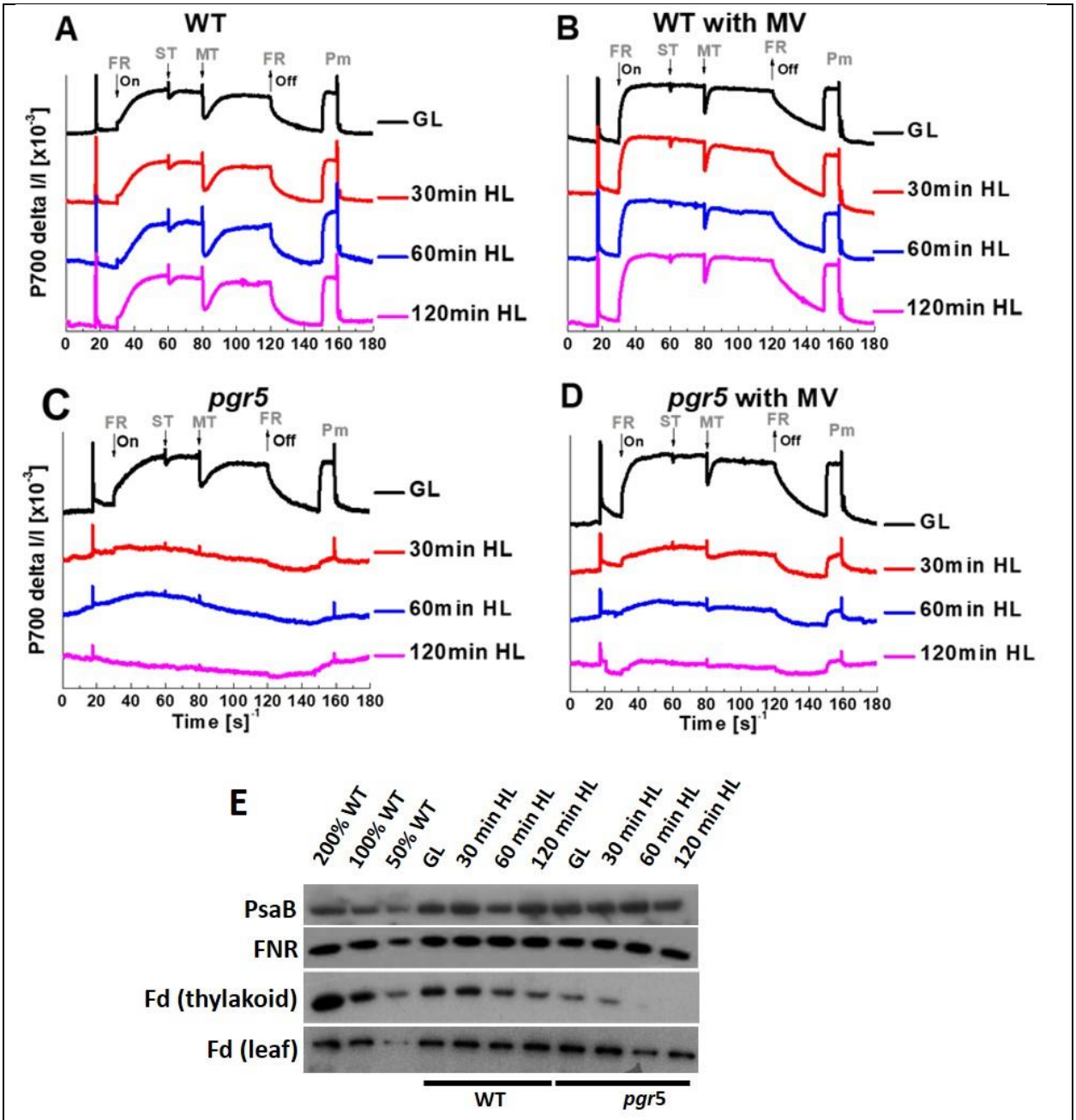

Figure 4: Photo-oxidation of P700 measured from GL- and HL-treated leaves in the presence and absence of MV, and changes in PsaB, FNR and Fd abundances during HL illumination of WT and

pgr5. **A-D**, Detached leaves of WT and the *pgr5* mutant plants, floating on water, were exposed to growth light (GL) (120 µmol photons m^{-2} s^{-1}) for 2-3h and then to high light (HL) (850 µmol photons m^{-2} s^{-1}, on the top of the leaves) for 30, 60 or 120 min. The oxidation of P700 was monitored in the background of far red (FR) light by applying single-turnover (ST) and multiple-turnover (MT) pulses of actinic light, followed by Pm measurements. **A**, WT leaves floating on deionized water n=6; **B**, WT leaves incubated with 1 µM MV for 2h in the dark before the measurements n=6; **C**, *pgr5* mutant leaves floating on deionized water n=6; **D**, *pgr5* mutant leaves incubated with 1 µM MV for 2h in the dark before the measurements n=6. **E,** Immunoblots of PsaB, FNR and Fd proteins from WT and *pgr5* leaves exposed to GL and HL. Gels were loaded with thylakoid samples based on equal Chl content (1 µg) (PsaB, FNR and Fd for thylakoids). For leaf total Fd analysis, the proteins were extracted from WT and *pgr5* leaves and the gels were loaded on equal protein basis (10 µg = 100%). Three biological replicates were simultaneously processed, and the WT GL samples were loaded as quantity controls (with 50%, 100% and 200% protein). Position of molecular weight markers with full scan of blots is available as extended data figure 3.

Similar to WT plants, the GL-grown *pgr5* plants showed faster oxidation of P700 in the presence of MV (**Fig. 4C,D**). However, the HL-treated *pgr5* leaves behaved differently. They showed a clear loss of photooxidation of P700 in FR light (**Fig. 4C**), as previously reported[16]. Only a modest increase in P700 oxidation was observed in HL-treated *pgr5* leaves upon firing actinic light in the background/absence of FR light (**Fig. 4C**). Furthermore, in the presence of MV, the HL-treated *pgr5* showed only a very low and slow oxidation of P700 in the continuous background of FR light (**Fig. 4D**). MV thus enhances P700 photooxidation in WT but fails to restore P700 photooxidation in HL-treated *pgr5* leaves, revealing a high amount of non-functional FeS_X clusters in *pgr5*. We therefore conclude that the FeS_X clusters were damaged nearly in parallel with $FeS_{A/B}$ in *pgr5*, but not in WT *Arabidopsis,* during the high HL treatment.

Ferredoxin depletes from thylakoids during HL treatment of leaves

To investigate additional effects on the acceptor side of PSI complexes upon HL illumination, the abundance of PsaB, FNR and Fd proteins from WT and *pgr5* mutant thylakoids was estimated by immunoblotting. While PsaB and FNR remained unchanged when WT and *pgr5* plants were transferred from GL to HL for up to 2 h, the differences in the abundance of thylakoid-bound Fd were evident (**Fig. 4E, and Extended_data_figure4**). The highest amount of thylakoid-bound Fd was detected in thylakoids isolated from GL-treated WT plants[25], whereas corresponding *pgr5* plants showed approximately 50% less of thylakoid-bound Fd compared to WT (**Fig. 4E**). HL treatment of plants for 30, 60 and 120 min resulted in a gradual decrease in thylakoid-associated Fd, which decreased in WT to approximately 50% of the pre-HL level and almost disappeared from the *pgr5* mutant thylakoids during the HL illumination of 120 min (**Fig. 4E**). This disappearance coincided with the severe loss of functional $FeS_{A/B}$ clusters in *pgr5* (**Fig. 2C**). To analyse whether the total Fd content or only the thylakoid-bound Fd decreased during the HL treatments, we also analysed the total leaf protein extracts by Fd immunoblotting. WT showed no decrease in Fd levels during the HL treatments and only a slight decrease in total Fd was observed in *pgr5* leaves after prolonged HL treatments (**Fig. 4E, and Extended_data_figure4**).

Superoxide production decreases in HL-treated leaves

It was previously hypothesized that PSI photoinhibition acts as a mechanism to prevent excessive ROS production in PSI[16,26] but no direct experimental evidence has so far been presented. Also, two electron transfer routes were recently reported to operate within PSI, one involved in forward electron transfer and the other in reverse reactions[1]. As the reverse reactions are likely to dissipate excess energy in HL, it is conceivable that they are enhanced upon the HL-treatment of leaves, thereby reducing ROS production in the forward route. To clarify this point, we next focused on measuring the net $O_2^{\bullet-}$ production capacity in thylakoids isolated from differentially light treated plants with different levels of PSI-photoinhibition. Thylakoids used in these experiments were isolated from WT and *pgr5* mutant plants, which were grown in GL or were HL-treated for 30, 60 and 120 min. The formation of $O_2^{\bullet-}$ was measured using 5 (diisopropoxyphosphoryl)-5-methyl-1-pyrroline-N-oxide 2-diisopropylphosphono-2-methyl-3,4-dihydro-2H-pyrrole-1-oxide spin trap (DIPPMPO) in the presence of low concentration (5 µM) of the chelator deferoxamine mysylate (desferol) to prevent formation of hydroxyl radicals from H_2O_2.

As shown in **Figure 5**, 30 min exposure of leaves to HL induced a 30 to 40% decline in $O_2^{\bullet-}$ production in both WT (**Fig. 5A**) and the *pgr5* mutant thylakoids (**Fig. 5C**). Extending the HL treatment of leaves to 60 min or 120 min had only a minor further effect on the decrease of $O_2^{\bullet-}$ production capacity of PSI in WT and *pgr5* (**Fig. 5A,C**). In contrast, addition of MV, an electron acceptor and thereby a putative extra $O_2^{\bullet-}$ producer, caused an increase in $O_2^{\bullet-}$ production in both WT and *pgr5* thylakoids isolated from GL-grown plants (comparison of the uppermost traces in **Fig. 5A,C** with the uppermost traces in **Fig. 5B,D**). Isolated thylakoids from WT leaves, HL-treated for 30, 60 and 120 mins, showed a similar enhancement in $O_2^{\bullet-}$ signal in each sample upon addition of MV (1 µM) (**Fig. 5B**) corresponding to that observed in thylakoids from GL leaves. Thus, the HL treatment of *Arabidopsis* WT leaves did not appear to change the capability of PSI to donate electrons to MV, occurring most likely via the FeS_X clusters. Interestingly, the HL treatment of *pgr5* leaves led to a completely different behavior of $O_2^{\bullet-}$ production in the presence of MV. In thylakoids isolated from the HL-treated *pgr5* mutant, the addition of MV did not cause any increase in the $O_2^{\bullet-}$ signal (**Fig. 5D**), opposite to that observed in *pgr5* thylakoids from GL leaves.

The above results on $O_2^{\bullet-}$ production in the presence and absence of MV strongly suggested that in GL as well as HL-treated WT but only in GL *pgr5* leaves ((**Fig. 5B,D**), MV is able to bypass the acceptor-side restriction within the internal PSI electron transfer chain caused by damage the $FeS_{A/B}$-clusters. In sharp contrast to WT and GL *pgr5*, the HL-treated *pgr5* mutant (**Fig. 5D**) was unable to increase $O_2^{\bullet-}$ production in the presence of MV. This result provided strong evidence that MV could not bypass the FeS_X clusters within the PSI electron transfer chain. However, there was a very low background production of $O_2^{\bullet-}$ in HL-treated plants, as shown by experiments with both WT **(Fig. 5A**, in the absence of MV) and *pgr5* (**Fig. 5B,** in the absence and presence of MV). We therefore postulate that such a small fraction of $O_2^{\bullet-}$ production occurs deeper within the PSI RC complex, without the involvement of electron transfer through any of the FeS clusters, as also suggested previously[27]. Importantly, the superoxide production experiments in WT and *pgr5* leaves (**Fig. 5**) strongly corroborate the respective P700 redox

measurements (Fig. 4), indicating that MV can only accept electrons from PSI via functional FeS_X clusters.

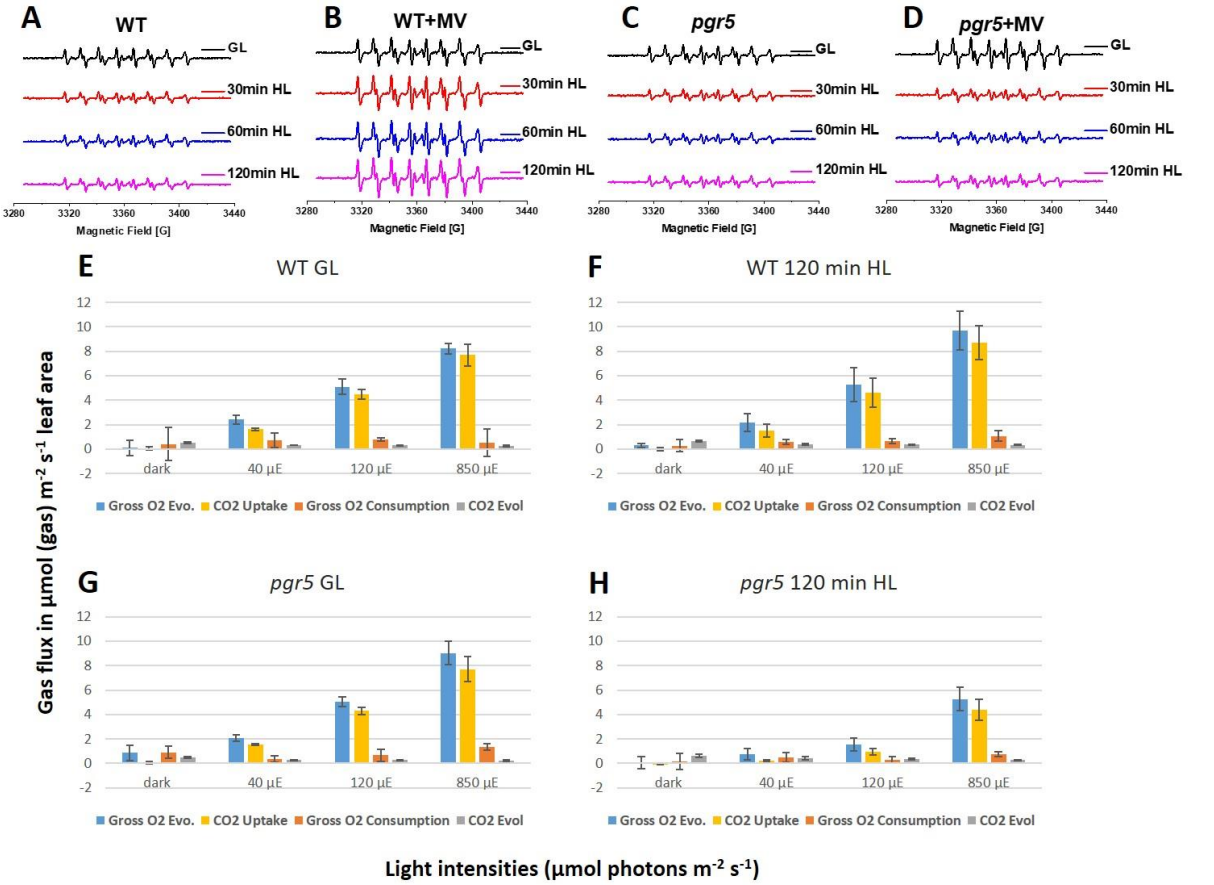

Figure 5. Superoxide production in isolated thylakoids and steady state gas flux measurements in leaf disks of GL- and HL-treated leaves. A, WT n=3. **B,** WT with MV (1 µM) n=3. **C,** *pgr5* mutant n=3. **D,** *pgr5* mutant with MV (1 µM) n=3. Superoxide production was measured with spin trap DIPPMPO in thylakoids isolated from plants exposed to growth light (GL) (120 µmol photons m^{-2} s^{-1}) for 2-3h and subsequently to high light (HL) (850 µmol photons m^{-2} s^{-1}) for 30, 60 or 120 min. The measurement conditions were microwave power 2 mW, centre field was 3363 G, and field sweep was 150 G. EPR spectra were obtained by 3 accumulations of each sample. **E-H,** The steady state gas flux was measured in leaf discs using MIMS. The atmosphere inside the MIMS cuvette (1ml volume) was enriched with two stable isotopes, $^{18}O_2$ and $^{13}CO_2$. The gas fluxes were measured in the dark and at given light intensities by collecting four masses 32, 36, 44 and 45 containing masses of naturally abundant isotopes. Leaf discs of 12.5 mm diameter were excised before turning on the lights in the phytotron from; **E,** GL-acclimated WT leaves n=3; **F,** 120 min HL-treated WT leaves n=3; **G**, GL-acclimated *pgr5* leaves n=3; and **H**, 120 min HL-treated *pgr5* leaves n=3. Gross O_2 evolution (blue bars) and gross O_2 consumption (orange bars), gross CO_2 uptake (yellow bars) and CO_2 consumption (grey bars) are shown in µmol (gas) exchange m^{-2} leaf area s^{-1}. The enriched CO_2 atmosphere minimized photorespiration, whilst a near-atmospheric O_2 level was maintained to maximize the likelihood of observing Mehler-associated O_2 reduction. Upon initiation of data acquisition, samples were first measured for four minutes in darkness, followed by five minutes of measurements at each light intensity (40, 120 and 850 µmol photons m^{-2} s^{-1}). Rates were calculated in each sample according to the equations described in[28]. Data are presented as mean values ±SD for (n) biological replicates.

FeS_X damage leads to a decrease in gas exchange rates in *pgr5*

The observation of PSI $FeS_{A/B}$ cluster damage induced by HL illumination in both the WT and *pgr5* mutant plants prompted us to investigate the relative effects of such a damage on leaf gas exchange rates (O_2 and CO_2). For this purpose, only the WT and *pgr5* leaves exposed to 120 min HL treatment, together with their GL control leaves, were subjected to gas exchange measurements by MIMS at four different light intensities (dark, 40 (LL), 120 (GL) and 850 µmol photons m^{-2} s^{-1} (HL)). CO_2 assimilation rates were determined by $^{13}CO_2$ enrichment, while the O_2 evolution and O_2 uptake rates were deconvoluted by measuring the isotope $^{16}O_2$ and the enriched isotope $^{18}O_2$, respectively. The rates of O_2 and CO_2 exchange measured over the four light intensities (dark, LL, GL and HL) of 2 h GL-acclimated plants, showed strong similarities between the WT and *pgr*5 leaves (**Fig. 5E,G**). In contrast, the 120 min HL treatment of intact WT and *pgr5* mutant leaves (**Fig. 5F,H**) resulted in very different responses between the WT and the *pgr5* mutant plants. WT *Arabidopsis* showed no decrease in O_2 and CO_2 exchange rates, but rather an increase in CO_2 uptake at 850 µmol photons m^{-2} s^{-1}. Instead, the *pgr5* mutant showed a substantial decrease in both the evolution of $^{16}O_2$ (naturally abundant isotope) and the uptake of $^{13}CO_2$ (artificially added carbon isotope) when measured at either 40, 120 or 850 µmol photons m^{-2} s^{-1}, whereas the O_2 photoreduction ($^{18}O2$ consumption) rather decreased in *pgr5* during 120 min HL exposure.

DISCUSSION

The susceptibility of PSI to photoinhibition under changing light conditions has been extensively studied, the *Arabidopsis* WT and *pgr5* mutants being probably the most widely investigated research targets[16,18,29–34]. The comparison here, focusing on the functionality of the electron transfer components from P700 oxidation to reduction of Fd, revealed major differences between WT and *pgr5* already in control plants from growth light conditions, a phenomenon rarely considered before. The *pgr5* plants showed much lower P700 oxidation (Pm) and $FeS_{A/B}$ reduction capacities compared to WT, whereas the functionality of PSII appeared equally efficient in both genotypes (**Fig. 1**). Although these differences between the two genotypes warrant further investigation of the role of the PGR5 protein under non-stressed conditions, we have focused here on HL conditions and mechanisms of PSI photoinhibition.

Based on P700 photooxidation and other functional characteristics of the PSI electron transfer components, we hypothesize here the existence of three distinct populations of PSI (**Figure 6 A,B,C**). These are the fully active type-I centres, the type-II centres, which are partially photoinhibited (the $FeS_{A/B}$ clusters are damaged but Pm remains unchanged) and type-III centres, which are severely photoinhibited with respect to P700 photooxidation, $FeS_{A/B}$ and FeS_X clusters. The abundance of different types of PSI centres in leaves is mainly determined by the light acclimation of the plant. Our results suggest that PSI does not limit photosynthesis in WT, since after the HL treatment the remaining fully functional PSI centres can easily carry out normal CO_2 fixation under all light conditions (**Fig. 5F**). However, in the *pgr5* mutant, all types of PSI are present already under GL and further shifts to type-II and type-III occur rapidly under HL illumination.

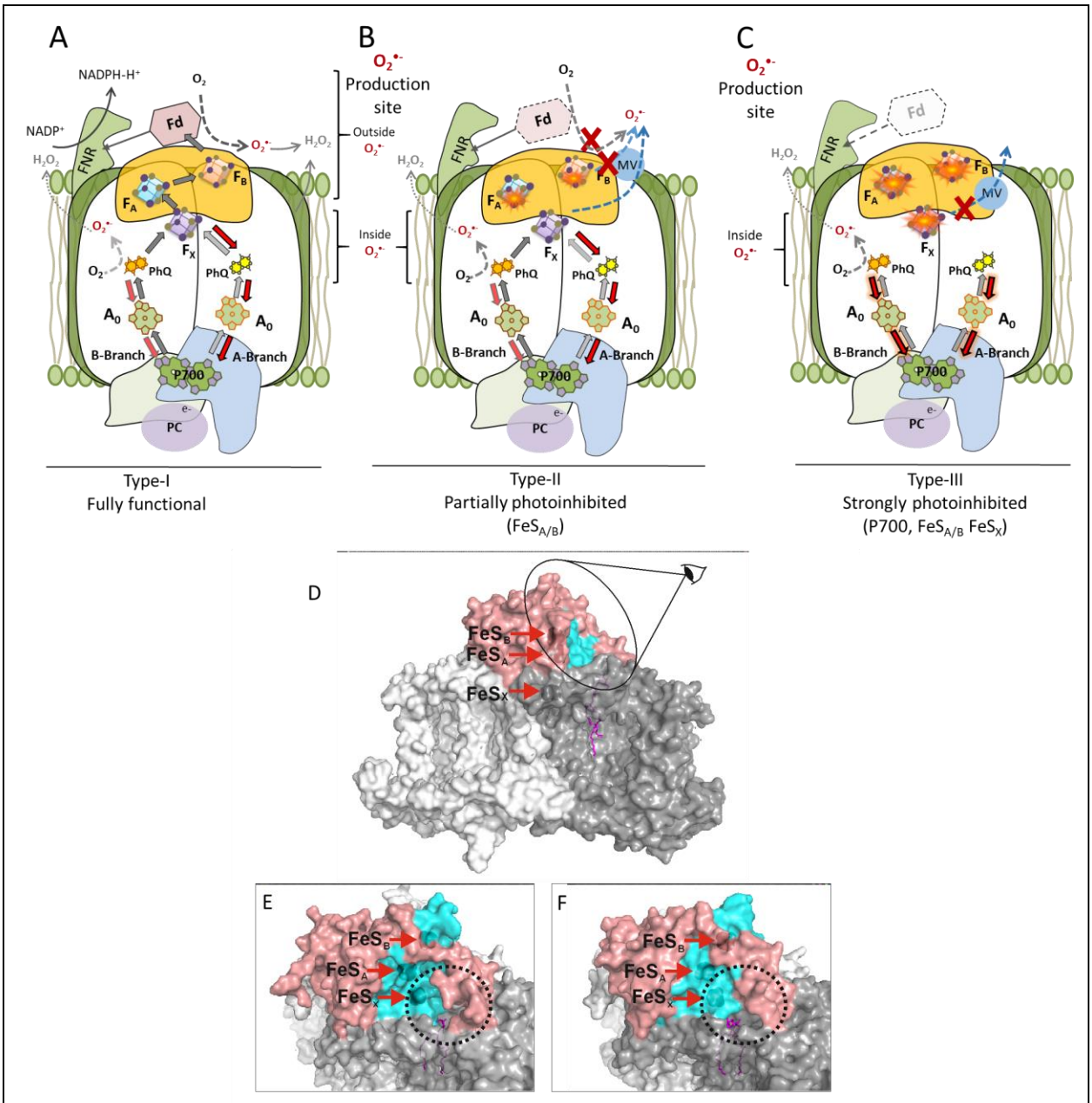

Figure 6. Schematic model showing the forward electron transfer steps and the back reaction pathways[1] in three types of PSI centres. A, Fully functional type-I PSI present in WT under GL, two possible sites for oxygen reduction in PSI are shown, one inside and one outside the complex. **B**, Partially photoinhibited type-II PSI centres with damaged $FeS_{A/B}$ clusters as observed in *pgr5* under GL and in WT only after HL treatment. The blue dotted arrow indicates sites where MV accepts electrons in PSI. **C**, strongly photoinhibited type-III PSI centres where electron transfer to MV is limited due to the damage of also the FeS_X clusters. The brightness and solid linings of the arrows emphasise the favored forward and backward electron transfer rates. **D-F,** Comparison of the PSI crystal structure obtained from isolations at pH 8.3 and 6.3, a view from the stromal surface showing the opening of a cavity between PsaB (grey), PsaC (cyan) and PsaD (pink) subunits. **D,** crystal structures at pH 8.3 from[55] Amunt et al. 2010; **E**, with a closer view of the opening shown in an inset; **F**, a closer view of the crystal structure at pH 6.3 from[56] Mazor et al. 2017.

PSI FeS clusters, in their natural state without excitation stress, i.e the type-I centres, have a strong preference either to reduce Fd via LET[35] or to allow protective back-reactions from FeS_X^- to $P700^+$ via the high potential PhQ^1 (**Fig.6A,** red arrow). However, clear symptoms of PSI photoinhibition started to appear as a gradual loss of the reduction capacity of $FeS_{A/B}$ clusters during the duration of the HL treatment (**Fig. 2B; Fig. 6B,** gradual appearance of type-II centres). This was not reflected in significant losses in the P700 oxidation (**Fig. 2A**) or FeS_X cluster reduction (**Fig. 4A**), thus still allowing stable P700 charge separation ($P700^+$ FeS_X^-). In these scenarios, the FeS_X^- plays a key role by either transferring electrons further, via the part of still functional $FeS_{A/B}$ clusters to Fd, or allowing a safe back reaction to re-reduce $P700^+$. Of the two electron transfer routes in PSI RC, the A-branch prefers back reactions, and the B-branch prefers the forward electron transfer to Fd[1]. Exceptionally long lifetime of the redox couples $P700^+FeS_A^-$ and $P700^+FeS_B^-$, *i.e.* 20 ms and 65 ms, respectively, provide relatively long time for back reactions to take place[36]. However, when the PSI acceptors are scarce and the PSI donor side (plastocyanin, PC) is highly reduced, the chances of back reactions are also lowered, and the damage to the $FeS_{A/B}$ clusters is expected (**Fig. 6B,** type-II reaction centres). Type-II centres, even if they remain non-functional for forward electron transfer, their appearance cannot be detected by Pm measurements. On the other hand, it has long been known that all functional PSI FeS clusters ($FeS_{A/B}^-$ and FeS_X^-) can donate electrons to MV, whereas PhQ^- lacks this ability due to redox hindrance[23,24,37]. Therefore, we can safely conclude that the maintenance of high Pm (**Fig. 4B**), despite a relatively high proportion (up to 50%) of non-functional $FeS_{A/B}$ clusters, implies that the FeS_X clusters remain functional in type-II reaction centres in WT *Arabidopsis* during the HL treatments applied here (**Fig. 6B**).

The integrity of the FeS clusters in HL in the p*gr5* mutant was very different from WT. The capacity of P700 photooxidation was severely compromised within 30 min HL illumination (low Pm after HL treatments; **Fig. 2**), which occurred in parallel with the loss of MV ability to accept electrons from PSI (**Figs. 4D,5D**), implying a severe damage of also the FeS_X clusters in *pgr5* **(Fig. 6C,** Type-III PSI centres**)**. The sequential damage of the $FeS_{A/B}^-$ and FeS_X^- clusters in *pgr5* most likely represents the situation that would also occur in WT *Arabidopsis* leaves if the HL conditions had lasted longer or the plants had been exposed to higher light intensities. Not only PSI but also PSII showed clear symptoms of photoinhibition in *pgr5* during HL treatment, although less severe compared to PSI photoinhibition, but PSII photoinhibition in WT was only marginal **Fig. 2**).

We also found a repair of PSI $FeS_{A/B}$ clusters in dim light (**Fig. 3**) after the HL treatments of 30, 60 and 120 min as an integral part of the regulatory network to balance the photosynthetic electron flow on the PSI acceptor side. The repair of type-II PSI centres with damaged $FeS_{A/B}$ clusters, however, appeared to be much slower than that generally known for optimal repair of photodamaged PSII complexes via D1 protein turnover[38,39] (about 15-30 min). Based on our results (Figs. 3 and 4E) we conclude that the replacement of damaged PSI core proteins may only occur after damage to FeS_X clusters, followed by the slow degradation of the entire PSI complex, which has been reported to take several days[19,22,40–43]. There is still an additional technical problem to analyse the repair of photoinhibited PSI, which arises from the fact that

although the PSI damage was severe (Type-II or III reaction centres, **Fig. 6B,C**) and a large part of photooxidisable P700s remained reduced, the operation of still functional PSI complexes (Type-I) is enhanced[19]. This compensatory mechanism allows a smaller number of fully active PSI centres (**Fig. 6A**) to maintain unchanged rates of LET to reduce Fd and maintain CO_2 fixation in WT *Arabidopsis*[44–46].

Our results revealed an interesting behavior of CO_2 fixation and ROS production in relation to the relatively frequent damage of PSI $FeS_{A/B}$ clusters in HL-treated WT *Arabidopsis* (**Fig. 2B**). Although the controlled damage of $FeS_{A/B}$ clusters does not seem to affect the CO_2 assimilation rates under low or moderately high light conditions (**Fig. 5F**) the damage clearly reduces the PSI ROS production (**Fig. 5A)**, i.e. the production of $O_2^{\bullet-}$radicals. It is therefore highly likely that the $FeS_{A/B}$ cluster damage acts as a protective mechanism against excessive ROS generation and immediate damage to FeS_X clusters and PSI core proteins under HL. The $FeS_{A/B}$ damage-related protection of PSI is supported by a slow repair mechanism (**Fig. 3**), which may involve only the replacement of damaged $FeS_{A/B}$ clusters in PSI, either by mechanisms involved in the assembly of chloroplast FeS clusters[47] or by as yet unidentified FeS cluster repair mechanisms similar to those reported in bacteria[48,49].
In contrast to WT, the more severe damage of PSI $FeS_{A/B}$ clusters during the HL treatment of the *pgr5* mutant (**Fig. 2B**) (**Fig. 6C**) resulted in impaired CO_2 fixation when measured under LL, GL or HL (**Fig. 5H**). This was reflected in a marked distortion of P700 oxidation kinetics (**Fig. 3F**) and persistently low production of ROS (**Fig. 5C,D**). In this case, FeS_X damage also occurred (**Fig. 5D**) and thylakoid-bound Fd[25] was depleted from the membrane (**Fig. 4E**). It is highly likely that such severe type-III PSI photodamage (**Fig. 6C**) represents the classic low-temperature PSI inhibition in chilling-sensitive angiosperms, leading to delayed degradation of the entire PSI complex[50]. Severe loss of entire PSI complexes also occurs in conifer chloroplasts during winter or early spring with concomitant distortion of P700 redox kinetics[51].

The severe damage of PSI $FeS_{A/B}$ clusters in the *pgr5* mutant (**Fig. 2B**), which also leads to damage of the FeS_X clusters, is in agreement with a recent report[52], showing that even when the lumen is acidified by CrPTOX2, the PGR5 protein is still required to oxidize P700. Thus, the protection of FeS clusters by the PGR5 protein, as evidenced by our results, also suggests that the PGR5-dependent trans-thylakoid pH gradient regulating electron transfer via the Cytb_6f is not sufficient to explain the specific role assigned here to PGR5 in protecting against FeS_X damage in WT. All other oxygenic photosynthetic organisms, except angiosperms, have solved the protection of PSI by using the FLV proteins as a protective valve to transfer electrons from reduced Fd to molecular oxygen when in excess, without generating ROS[53]. The introduction of moss *FlvA* and *FlvB* genes into *Arabidopsis* fully complemented the oxidation of P700 in the *pgr5* background[54], suggesting that they are also functional in *Arabidopsis*. However, angiosperms have lost the *flv* genes during evolution, apparently to avoid the loss of energy already stored in light reactions, and have evolved another mechanism that relies heavily, but not completely, on PGR5.

Interestingly, the comparison of the two PSI crystal structures from angiosperms revealed an apparent degree of flexibility in the packing at the stromal interface of the PsaC, PsaD and PsaB

subunits (**Fig. 6D-F**), which host the $FeS_{A/B}$ clusters. As shown in **Figure 6E**, the PSI crystal isolated at pH 8.3 (PDB 5L8R)[55] has an opening in the region of Asp552 and Phe553 (PsaB), Tyr68 and Trp70 (PsaC) and Gln207 (PsaD) that was not seen in crystals isolated at pH 6.3 (PDB 3LW5)(**Fig. 6F**)[56]. Such a flexibility in this region of the PSI structure could alter the electron transfer between the FeS clusters on the acceptor side of PSI in a pH-dependent manner. In such a case, a strong pH gradient supported by PGR5 would maintain the structure with the opening for electron transfer, whereas in the *pgr5* mutant the "closed" PSI structure is favoured. It is therefore conceivable that the absence of the PGR5 protein not only affects the Cytb_6f electron transfer but also modulates the PSI structure, thereby contributing to the protection of the FeS_X clusters and avoidance of severe PSI photoinhibition.

Overall, our results suggest that PSI FeS clusters in angiosperm chloroplasts are susceptible to over-reduction and photodamage in high light. The PSI FeS cluster damage may occur frequently in high light similar to that of PSII damage, but is not observable by gas exchange or P700 spectroscopic methods. Conversely, we suggest that photodamage of PSI $FeS_{A/B}$ clusters in *Arabidopsis* plays an important role in the HL tolerance of the photosynthetic light reactions. PSI $FeS_{A/B}$ damage occurs during HL exposure of leaves through a tightly choreographed chain of feedback reactions, and maintains maximum electron flux through LET. On the one hand, the photodamaged PSI $FeS_{A/B}$ clusters prevent excessive electron transfer from LET to O_2 and, simultaneously, the enhanced kinetics of PSI photochemistry in undamaged centres ensures an almost unchanged capacity for CO_2 assimilation over a range of light intensities. This mechanism ensures that flowering plants maintain CO_2 assimilation at rates close to those of undamaged PSI plants, while minimising the risk of excessive production of reactive O_2 species, which have the potential to cause further damage. Nevertheless, a limited loss of PSI $FeS_{A/B}$ clusters, as observed in WT *Arabidopsis*, can only compensate for a reasonable imbalance in LET. In fact, an extreme imbalance in LET, such as that observed in *pgr5* mutant plants, leads to severe damage also to the PSI FeS_X clusters, ultimately rendering the *pgr5* mutant unable to survive under the given light conditions.

Methods

Plant material – Trichomeless *Arabidopsis thaliana* ecotype Columbia-0 wild-type (WT) *glabra1* and the *pgr5* mutant[32], were grown on soil at 24°C for 6 weeks in an 8 h photoperiod with a light intensity 120 µmol photons m^{-2} s^{-1} (GL). Leaves were detached 2-3h into the photoperiod, floated on distilled water and transferred to HL (850 µmol photons m^{-2} s^{-1}) for 30, 60 or 120 min. Chloroplasts were than isolated from light treated fresh leaves[16]. Briefly, leaves were homogenized in buffer containing 330 mM sorbitol, 5 mM EDTA, 5 mM EGTA, 5 mM $MgCl_2$, 50 mM Hepes/KOH (pH 7.5), with freshly added 5 mM sodium ascorbate, 0.5% (w/v) fatty acid-free BSA and 5 mM NaF. The suspension was filtered and centrifuged at 3000 ×g for 6 min at 4°C. The pellet was resuspended and washed twice in buffer containing 100 mM sorbitol, 10 mM $MgCl_2$, 50 mM Hepes (pH 7.5), and stored at -80°C until further use. The chloroplast envelope if remained intact was broken by freeze/thawing of the samples.

Measurements of LET and gas exchange – We performed mass spectrometric gas exchange measurements on leaf discs cut from detached leaves as previously described[57,58]. Briefly, fresh leaf discs were cut from dark-adapted detached leaves and loaded into a home-made stainless steel cuvette of 1

ml volume, equilibrated and calibrated at 25 °C, using a Teflon membrane (Hansatech) membrane to separate the sample chamber from the high vacuum line of mass spectrometer. In darkness, the endogenous $^{12}CO_2$ was purged from the samples by flushing with compressed atmospheric air without $^{12}CO_2$ (Soda Lime, Li-Core, USA), then the cuvette was enriched to approximately 2% by volume $^{13}CO_2$ and 3% by volume $^{18}O_2$, with the remainder of the atmosphere containing approximately standard atmospheric concentrations. The very low partial pressure of $^{12}CO_2$ at the beginning of measurements minimized membrane consumption of this isotope to almost zero, allowing the rate of its production in the dark (mitochondrial respiration) to be used as a basis for setting the background consumption rate of $^{18}O_2$ (mitochondrial respiration in dark, plus Mehler reaction during illumination). The rates of $^{16}O_2$ (PSII water splitting) and $^{13}CO_2$ (CO_2 assimilation by Rubisco) were both set to zero in the dark. The enriched CO_2 atmosphere avoided photorespiration, while a near-atmospheric O2 level was maintained to maximise the likelihood of observing Mehler-associated O2 reduction, with the same offsets for steady dilution of stable isotopes used in steady-state flux calculations as described previously [57,58]. The discs were kept in the dark in the cuvette for approximately five minutes to ensure isotopic equilibrium in the system prior to measurement. The instrument recorded m/z 32, 36, 44 and 46 with a time resolution of approximately 6.5 seconds. After four minutes of darkness, a halogen light directed through a liquid light guide illuminated the samples at 40, 120 and then 850 µmol photons m-2 s-1. All data were analysed and fluxes calculated using equations described in Beckmann et al[28]. Leaf discs are often used as a surrogate for intact leaf measurements. Although there are experimental limitations regarding altered physiological responses between a leaf disc and an intact leaf, for the purpose of demonstrating functional PSI activity via CO2 assimilation, these limitations do not apply to this set of experiments.

Redox changes in PSI and PSII fluorescence – The determination of functional PSII and PSI was performed on detached intact leaves using a saturating pulse method on Dual-PAM-100 (Walz, Germany) as described previously[16].

FeS clusters measurements– The FeS clusters ($FeS_{A/B}$) were analyzed by low temperature EPR measurements in isolated thylakoids from GL and HL treated WT and *pgr5* plants at 16 K as described previously[16].

Western blotting – Isolated thylakoids equivalent to 0,5 µg Chl were separated by SDS-PAGE (12% polyacrylamide, 6 M urea)[59]. Proteins were electrotransferred to a polyvinyledine fluoride membrane (Immobilon-P, Millipore). Western blotting was performed using standard techniques with the antibodies Fd (Agrisera, AS06 121), FNR (Agrisera, AS15 2909) and PsaB (Agrisera, AS10 695). The enhanced luminol-based chemiluminescent substrate system (ECL, abcam) was used for visualization. Quantification was performed using AlphaEaseFC software (Fluor Cam 8000).

Superoxide measurements – Spin trapping for $O_2^{\bullet -}$ was performed in isolated thylakoids from GL-grown and HL-treated WT and *pgr5* plants using a Miniscope (MS5000) EPR spectrometer equipped with a variable temperature controller (TC-HO4) and a Hamamatsu light source (LC8). Isolated thylakoids equivalent to 15 µg ml^{-1} Chl were exposed to actinic light (2000 µmol photons m^{-2} s^{-1}) for 180 s in the presence of 50 mM Hepes-NaOH (pH 7.5), 50 µM desferol with 5-(Diisopropoxyphosphoryl)-5-methyl-1-pyrroline-N-oxide; 2-Diisopropylphosphono-2-methyl-3,4-dihydro-2H-pyrrole-1-oxide (DIPPMPO) spin trap (50 mM). The samples were then centrifuged at 6500×g for 5 min and the supernatant was used for EPR measurements. Measurements were performed at frequency 9.41 GHz, centre field 3363 G, field sweep of 150 G, microwave power of 3 mW and modulation frequency of 100 kHz with a modulation width of 2G. Final spectra were obtained from 5 accumulations of each sample.

Data Availability: All raw data is available for this paper at figshare.

https://figshare.com/articles/dataset/_/26273044

Acknowledgement: Jane and Aatos Erkko Foundation is acknowledged for financial support (2020-2024). We thank Prof. Nathan Nelson for providing the crystal structure data and Dr. Peter Gollan for preparing figure from crystal structure data.

Author Contributions: AT, MT and E-MA designed and conceptualized the work. The experimental work was performed by AT, FM, DF and SG. Results were analyzed by AT, FM, DF, SG, MT and E-MA, and the manuscript was written by AT, MT and E-MA. All authors participated in revision of the manuscript.

Competing Interests: Authors declare no competing interests.

References:

1. Rutherford, A. W., Osyczka, A. & Rappaport, F. Back-reactions, short-circuits, leaks and other energy wasteful reactions in biological electron transfer: Redox tuning to survive life in O 2. *FEBS Letters* vol. 586 603–616 (2012).
2. Asada, K. *THE WATER-WATER CYCLE IN CHLOROPLASTS: Scavenging of Active Oxygens and Dissipation of Excess Photons*. *Annu. Rev. Plant Physiol. Plant Mol. Biol* vol. 50 (1999).
3. Dietz, K. J., Mittler, R. & Noctor, G. Recent progress in understanding the role of reactive oxygen species in plant cell signaling. *Plant Physiology* vol. 171 1535–1539 (2016).
4. Noctor, G., Reichheld, J.-P. & Foyer, C. H. ROS-related redox regulation and signaling in plants. *Semin. Cell Dev. Biol.* **80**, 3–12 (2018).
5. Ilík, P. *et al.* Alternative electron transport mediated by flavodiiron proteins is operational in organisms from cyanobacteria up to gymnosperms. *New Phytol.* **214**, 967–972 (2017).
6. Zhang, P., Allahverdiyeva, Y., Eisenhut, M. & Aro, E.-M. Flavodiiron Proteins in Oxygenic Photosynthetic Organisms: Photoprotection of Photosystem II by Flv2 and Flv4 in Synechocystis sp. PCC 6803. *PLoS One* **4**, e5331 (2009).
7. Miyake, C. Alternative electron flows (water-water cycle and cyclic electron flow around PSI) in photosynthesis: Molecular mechanisms and physiological functions. *Plant and Cell Physiology* vol. 51 1951–1963 (2010).
8. Yamori, W. & Shikanai, T. Physiological Functions of Cyclic Electron Transport Around Photosystem I in Sustaining Photosynthesis and Plant Growth. *Annu. Rev. Plant Biol.* **67**, 81–106 (2016).
9. Nishikawa, Y. *et al.* PGR5-dependent cyclic electron transport around PSI contributes to the redox homeostasis in chloroplasts rather than CO2 fixation and biomass production in rice. *Plant Cell Physiol.* **53**, 2117–2126 (2012).
10. Yang, Y. J., Ding, X. X. & Huang, W. Stimulation of cyclic electron flow around photosystem I upon a sudden transition from low to high light in two angiosperms Arabidopsis thaliana and Bletilla striata. *Plant Sci.* **287**, (2019).
11. Niyogi, K. K. Safety valves for photosynthesis. *Curr. Opin. Plant Biol.* **3**, 455–460 (2000).
12. Holzwarth, A. R. & Jahns, P. Non-Photochemical Quenching Mechanisms in Intact

Organisms as Derived from Ultrafast-Fluorescence Kinetic Studies. in *Non-Photochemical Quenching and Energy Dissipation in Plants, Algae and Cyanobacteria* (eds. Demmig-Adams, B., Garab, G., Adams III, W. & Govindjee) 129–156 (Springer Netherlands, 2014). doi:10.1007/978-94-017-9032-1_5.

13. Tikkanen, M., Rantala, S., Grieco, M. & Aro, E. M. Comparative analysis of mutant plants impaired in the main regulatory mechanisms of photosynthetic light reactions - From biophysical measurements to molecular mechanisms. *Plant Physiol. Biochem.* **112**, 290–301 (2017).
14. Tikhonov, A. N., Khomutov, G. B., Ruuge, E. K. & Blumenfeld, L. A. Electron transport control in chloroplasts. Effects of photosynthetic control monitored by the intrathylakoid pH. *Biochim. Biophys. Acta - Bioenerg.* **637**, 321–333 (1981).
15. Foyer, C. H., Neukermans, J., Queval, G., Noctor, G. & Harbinson, J. Photosynthetic control of electron transport and the regulation of gene expression. *Journal of Experimental Botany* vol. 63 1637–1661 (2012).
16. Tiwari, A. *et al.* Photodamage of iron–sulphur clusters in photosystem I induces non-photochemical energy dissipation. *Nat. Plants* **2**, 16035 (2016).
17. Huang, W., Tikkanen, M. & Zhang, S. B. Photoinhibition of photosystem I in Nephrolepis falciformis depends on reactive oxygen species generated in the chloroplast stroma. *Photosynth. Res.* **137**, 129–140 (2018).
18. Tikkanen, M., Rantala, S. & Aro, E. M. Electron flow from PSII to PSI under high light is controlled by PGR5 but not by PSBS. *Front. Plant Sci.* **6**, (2015).
19. Lempiäinen, T., Rintamäki, E., Aro, E. & Tikkanen, M. Plants acclimate to Photosystem I photoinhibition by readjusting the photosynthetic machinery. *Plant. Cell Environ.* **45**, 2954–2971 (2022).
20. Porcar-Castell, A. A high-resolution portrait of the annual dynamics of photochemical and non-photochemical quenching in needles of Pinus sylvestris. *Physiol. Plant.* **143**, 139–153 (2011).
21. Briantais, J.-M., Dacosta, J., Goulas, Y., Ducruet, J.-M. & Moya, I. Heat stress induces in leaves an increase of the minimum level of chlorophyll fluorescence, Fo: A time-resolved analysis. *Photosynth. Res.* **48**, 189–196 (1996).
22. Lima-Melo, Y., Gollan, P. J., Tikkanen, M., Silveira, J. A. G. & Aro, E. Consequences of photosystem-I damage and repair on photosynthesis and carbon use in *Arabidopsis thaliana*. *Plant J.* **97**, 1061–1072 (2019).
23. Fujii, T., Yokoyama, E.-I., Inoue, K. & Sakurai, H. *The sites of electron donation of Photosystem I to methyl viologen*. *Biochimica et Biophysica Acta* (1990).
24. Milanovsky, G. E., Petrova, A. A., Cherepanov, D. A. & Semenov, A. Y. Kinetic modeling of electron transfer reactions in photosystem I complexes of various structures with substituted quinone acceptors. *Photosynth. Res.* **133**, 185–199 (2017).
25. Utschig, L. M., Duckworth, C. L., Niklas, J. & Poluektov, O. G. EPR studies of ferredoxin in spinach and cyanobacterial thylakoids related to photosystem I-driven NADP+ reduction. *Photosynth. Res.* (2024) doi:10.1007/s11120-023-01072-4.
26. Takagi, D. *et al.* Diversity of strategies for escaping reactive oxygen species production within photosystem I among land plants: P700 oxidation system is prerequisite for alleviating photoinhibition in photosystem I. *Physiol. Plant.* **161**, 56–74 (2017).

27. Kozuleva, M. A., Petrova, A. A., Mamedov, M. D., Semenov, A. Y. & Ivanov, B. N. O 2 reduction by photosystem I involves phylloquinone under steady-state illumination. *FEBS Lett.* **588**, 4364–4368 (2014).
28. Beckmann, K., Messinger, J., Badger, M. R., Wydrzynski, T. & Hillier, W. On-line mass spectrometry: membrane inlet sampling. *Photosynth. Res.* **102**, 511–522 (2009).
29. Suorsa, M. *et al.* PGR5 ensures photosynthetic control to safeguard photosystem I under fluctuating light conditions. *Plant Signal. Behav.* **8**, e22741 (2013).
30. Yamamoto, H. & Shikanai, T. Does the Arabidopsis proton gradient regulation5 Mutant Leak Protons from the Thylakoid Membrane?1[OPEN]. *Plant Physiol.* **184**, 421–427 (2020).
31. Zhou, Q., Yamamoto, H. & Shikanai, T. Distinct contribution of two cyclic electron transport pathways to P700 oxidation. *Plant Physiol.* **192**, 326–341 (2023).
32. Munekage, Y. *et al.* PGR5 is involved in cyclic electron flow around photosystem I and is essential for photoprotection in Arabidopsis. *Cell* **110**, 361–71 (2002).
33. Rantala, S. *et al.* PGR5 and NDH-1 systems do not function as protective electron acceptors but mitigate the consequences of PSI inhibition. *Biochim. Biophys. Acta - Bioenerg.* **1861**, (2020).
34. Takagi, D. & Miyake, C. PROTON GRADIENT REGULATION 5 supports linear electron flow to oxidize photosystem I. *Physiol. Plant.* **164**, 337–348 (2018).
35. Munekage, Y. N., Genty, B. & Peltier, G. Effect of PGR5 Impairment on Photosynthesis and Growth in Arabidopsis thaliana. *Plant Cell Physiol.* **49**, 1688–1698 (2008).
36. Vassiliev, I. R., Antonkine, M. L. & Golbeck, J. H. Iron–sulfur clusters in type I reaction centers. *Biochim. Biophys. Acta - Bioenerg.* **1507**, 139–160 (2001).
37. Petrova, A. A. *et al.* Interaction of various types of photosystem I complexes with exogenous electron acceptors. *Photosynth. Res.* **133**, 175–184 (2017).
38. Aro, E.-M., Virgin, I. & Andersson, B. Photoinhibition of Photosystem II. Inactivation, protein damage and turnover. *Biochim. Biophys. Acta - Bioenerg.* **1143**, 113–134 (1993).
39. Nishiyama, Y., Allakhverdiev, S. I. & Murata, N. Protein synthesis is the primary target of reactive oxygen species in the photoinhibition of photosystem II. *Physiol. Plant.* **142**, 35–46 (2011).
40. Kudoh, H. & Sonoike, K. Irreversible damage to photosystem I by chilling in the light: cause of the degradation of chlorophyll after returning to normal growth temperature. *Planta* **215**, 541–548 (2002).
41. Li, X. G., Wang, X. M., Meng, Q. W. & Zou, Q. Factors Limiting Photosynthetic Recovery in Sweet Pepper Leaves After Short-Term Chilling Stress Under Low Irradiance. *Photosynthetica* **42**, 257–262 (2004).
42. Bernhard Teicher, H., Lindberg Møller, B. & Vibe Scheller, H. Photoinhibition of Photosystem I in field-grown barley (Hordeum vulgare L.): Induction, recovery and acclimation. *Photosynth. Res.* **64**, 53–61 (2000).
43. Schöttler, M. A., Albus, C. A. & Bock, R. Photosystem I: Its biogenesis and function in higher plants. *J. Plant Physiol.* **168**, 1452–1461 (2011).
44. Schöttler, M. A., Tóth, S. Z., Boulouis, A. & Kahlau, S. Photosynthetic complex stoichiometry dynamics in higher plants. *Source J. Exp. Bot.* **66**, 2373–2400 (2015).
45. Shimakawa, G. & Miyake, C. What Quantity of Photosystem I Is Optimum for Safe

Photosynthesis? *Plant Physiol.* **179**, 1479–1485 (2019).
46. Ermakova, M. *et al.* Upregulation of bundle sheath electron transport capacity under limiting light in C4 Setaria viridis. *Plant J.* **106**, 1443–1454 (2021).
47. Lu, Y. Assembly and Transfer of Iron–Sulfur Clusters in the Plastid. *Front. Plant Sci.* **9**, (2018).
48. Djaman, O., Outten, F. W. & Imlay, J. A. Repair of Oxidized Iron-Sulfur Clusters in Escherichia coli. *J. Biol. Chem.* **279**, 44590–44599 (2004).
49. Keyer, K. & Imlay, J. A. Inactivation of Dehydratase [4Fe-4S] Clusters and Disruption of Iron Homeostasis upon Cell Exposure to Peroxynitrite. *J. Biol. Chem.* **272**, 27652–27659 (1997).
50. Sonoike, K., Terashima, I., Iwaki, M. & Itoh, S. Destruction of photosystem I iron-sulfur centers in leaves of Cucumis sativus L. by weak illumination at chilling temperatures. *FEBS Lett.* **362**, 235–238 (1995).
51. Grebe, S. & Porcar-castell, Albert; Riikonen, Anu; Paakkarinen, Virpi; Aro, E.-M. *Accounting for photosystem I photoinhibition sheds new light on seasonal acclimation strategies of boreal conifers*. vol. Inpress (Journal of Experimental Botany, 2023).
52. Zhou, Q., Wang, C., Yamamoto, H. & Shikanai, T. PTOX-dependent safety valve does not oxidize P700 during photosynthetic induction in the Arabidopsis pgr5 mutant. *Plant Physiol.* **188**, 1264–1276 (2022).
53. Allahverdiyeva, Y. *et al.* Flavodiiron proteins Flv1 and Flv3 enable cyanobacterial growth and photosynthesis under fluctuating light. *Proc. Natl. Acad. Sci.* **110**, 4111–4116 (2013).
54. Yamamoto, H., Takahashi, S., Badger, M. R. & Shikanai, T. Artificial remodelling of alternative electron flow by flavodiiron proteins in Arabidopsis. *Nat. Plants* **2**, (2016).
55. Amunts, A., Toporik, H., Borovikova, A. & Nelson, N. Structure determination and improved model of plant photosystem I. *J. Biol. Chem.* **285**, 3478–3486 (2010).
56. Mazor, Y., Borovikova, A., Caspy, I. & Nelson, N. Structure of the plant photosystem i supercomplex at 2.6 Å resolution. *Nat. Plants* **3**, (2017).
57. Fitzpatrick, D., Aro, E.-M. & Tiwari A., A. A Commonly Used Photosynthetic Inhibitor Fails to Block Electron Flow to Photosystem I in Intact Systems. *Front. Plant Sci.* **11**, (2020).
58. Fitzpatrick, D., Aro, E.-M. & Tiwari, A. True oxygen reduction capacity during photosynthetic electron transfer in thylakoids and intact leaves. *Plant Physiol.* **189**, 112–128 (2022).
59. Laemmli, U. K. Cleavage of Structural Proteins during the Assembly of the Head of Bacteriophage T4. *Nature* **227**, 680–685 (1970).